HHS Public Access

Author manuscript

ACS Chem Biol. Author manuscript; available in PMC 2022 July 16.

Published in final edited form as:

ACS Chem Biol. 2021 July 16; 16(7): 1234–1242. doi:10.1021/acschembio.1c00279.

Chemoproteomic study uncovers HemK2/KMT9 as a new target for NTMT1 bisubstrate inhibitors

Dongxing Chen[†], **Ying Meng**[†], **Dan Yu**[‡], **Nicholas Noinaj**[§], **Xiaodong Cheng**[‡], **Rong Huang**[*,†]

[†]Department of Medicinal Chemistry and Molecular Pharmacology, Purdue Institute for Drug Discovery, Purdue University Center for Cancer Research, Purdue University, West Lafayette, Indiana 47907, United States

[§]Department of Biological Sciences, Markey Center for Structural Biology, and the Purdue Institute of Inflammation, Immunology and Infectious Disease, Purdue University, West Lafayette, Indiana 47907, United States

[‡]Department of Epigenetics and Molecular Carcinogenesis, University of Texas M.D. Anderson Cancer Center, Houston, Texas 77030, United States

Abstract

Understanding the selectivity of methyltransferase inhibitors is important to dissect the functions of each methyltransferase target. From this perspective, here we report a chemoproteomic study to profile the selectivity of a potent protein N-terminal methyltransferase 1 (NTMT1) bisubstrate inhibitor NAH-C3-GPKK ($K_{i,\ app}$ = 7±1 nM) in endogenous proteomes. First, we describe the rational design, synthesis, and biochemical characterization of a new chemical probe **6**, a biotinylated analogue of NAH-C3-GPKK. Next, we systematically analyze protein networks that may selectively interact with the biotinylated probe **6** in concert with the competitor NAH-C3-GPKK. Besides NTMT1, the designated NTMT1 bisubstrate inhibitor NAH-C3-GPKK was found to also potently inhibit a methyltransferase complex HemK2-Trm112 (also known as KMT9-Trm112), highlighting the importance of systematic selectivity profiling. Furthermore, this is the first potent inhibitor for HemK2/KMT9 as reported by now. Thus, our studies lay the foundation for future efforts to develop selective inhibitors for either methyltransferase.

Graphical Abstract

[*]**Corresponding Author:** Phone: (765) 494 3426. huang-r@purdue.edu.

Author Contributions

R.H. conceived and directed the project. R.H. and D.C. designed the compounds. D.C. synthesized, purified, and characterized the compounds. D.C. purified NTMT1 and performed co-crystallization. N.N. collected X-ray diffraction data and refined the co-crystal structure. Y.M. performed the pull-down study and bioinformatic analysis. X.C. supervised and D.Y. characterized the inhibition study for HemK2-Trm112 and MettL5-Trm112. D.C. and Y.M. wrote the manuscript. R.H. and X.C. edited the manuscript. All authors provided critical feedback and have approved the final version of the manuscript.

Supporting Information

MS and HPLC analysis of compounds **1**-**6**; Figure S1. IC_{50} curves for compounds **1** and **5**, respectively; Figure S2. Pull-down studies with recombinant NTMT1 and HemK2-Trm112 complex from immobilized probe **6**; Table S1. Proteomic analysis of HeLa cell proteomics enriched by probe **6** through LC-MS/MS; Table S2. Crystallography data and refinement statistics (PDB ID: 6PVA).

Accession Codes

The coordinates for the structure of human NTMT1 in complex with compound **NAH-C3-GPKK (**PDB ID: 6PVA) has been deposited in the Protein Data Bank.

The authors declare no competing financial interest.

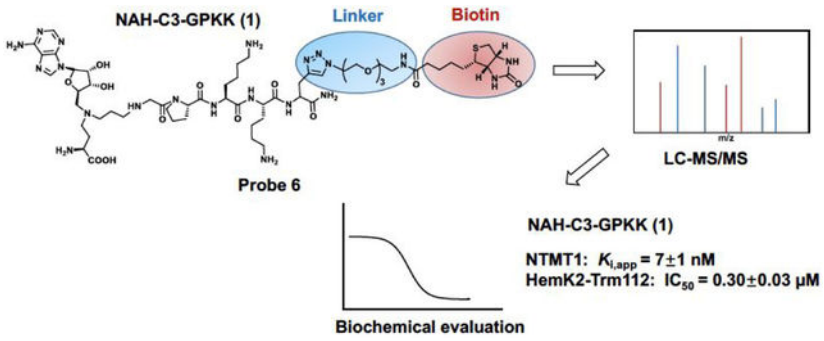

INTRODUCTION

Protein methylation regulates numerous biological processes, including transcription, DNA repair, and RNA metabolism.[1–3] Protein methyltransferases (MTs) are the enzymes that catalyze the transfer of a methyl group from the cofactor S-adenosyl-L-methionine (SAM) onto protein substrates. The substrate preference of MTs determines their respective functions and annotations.[4–10] For example, protein N-terminal MTs (NTMTs), lysine MTs (PKMTs), and arginine MTs (PRMTs) catalyze the methylation on protein α-N-termini, ε-amino group of the lysine, and guanidinium nitrogen atoms of the arginine, respectively.[4–10] As the dysregulation of MTs has been implicated in various diseases, selectivity of the inhibitors is essential to elucidate the physiological and pharmacological functions of the MTs.[1–3,11–13]

NTMT1 methylates the protein α-N-terminal amines of a specific motif X-P-K/R, where X represents any amino acid other than D/E.[5,8,14] Substrates of NTMT1 include centromere H3 variants CENP-A/B, the regulator of chromatin condensation 1 (RCC1), damaged DNA-binding protein 2, poly(ADP-ribose) polymerase 3, and transcription factor-like protein MRG15.[5,15–18] Recent progress has revealed the important role of NTMT1 in chromosome segregation, mitosis, and DNA damage repair.[18–20] Knockdown of NTMT1 sensitized the breast cancer cell lines to etoposide and γ irradiation treatment, and knockout of NTMT1 resulted in developmental defects and premature aging in mice.[20,21] Therefore, such critical cellular processes highlight the need for the development of highly selective chemical probes for NTMT1. Towards this goal, we have previously developed a series of potent NTMT1 bisubstrate inhibitors by covalently linking the SAM mimic with a peptide substrate to allow them to simultaneously occupy neighboring binding sites of SAM and substrate. Two representative examples are NAH-C3-PPKRIA ($K_{i,\ app}$ = 39±10 nM) and NAH-C4-GPKRIA ($K_{i,\ app}$ = 0.13±0.04 nM) (Figure 1), where NAH is a SAM mimic by replacing the sulfonium ion with a nitrogen atom. Meanwhile, they displayed selectivity over two representative PKMTs (G9a and SETD7) and three PRMTs (PRMT1, 3, and 7) in the biochemical assays.[22–25] Furthermore, NAH-C4-GPKRIA exhibits selective for NTMT1 over its closely related homolog NTMT2, suggesting the unique active site of NTMT1 and high selectivity of NTMT1 bisubstrate inhibitors.[25] While NTMT1 bisubstrate inhibitors exhibit decent selectivity among multiple MTs against isolated enzymes in biochemical assays, there is no information on any other targets that those inhibitors may interact within

cellular contexts to understand any off-target engagement and delineate the mechanism of action.

Chemoproteomic profiling is a powerful approach to provide a global insight into the cellular targets of an inhibitor in a complex biological environment by utilizing immobilized or photoreactive inhibitors. Here, we design and synthesize a biotinylated derivative of NTMT1 bisubstrate inhibitor **1** (NAH-C3-GPKK) to generate probe **6** (NAH-C3-GPKK-biotin), allowing it to be immobilized with streptavidin beads. Following pull-down study of probe **6** confirms its ability to efficiently enrich NTMT1 from the whole cell lysates. In addition, probe **6** also binds to another protein methyltransferase, i.e. HemK2-Trm112 complex (also known as KMT9 -Trm112), that methylates both lysines of histone H4 and glutamine of the eukaryotic release factor 1 (eRF1).[4,26] Subsequent validation confirms that compound **1** acts as a dual potent inhibitor for NTMT1 and HemK2/KMT9. To our knowledge, this is the first inhibitor reported for HemK2/KMT9, which offers a new revenue for the use of this compound.

RESULTS AND DISCUSSION

Design and synthesis.

To design the optimal probe for the selectivity profiling of NTMT1 bisubstrate inhibitors, we first investigate the structure-activity relationship (SAR) of the NTMT1 bisubstrate inhibitors. Thus, we synthesized new bisubstrate analogues **1**-**4** with different peptide sequences and variable linkers to choose the optimal position to install a biotin group. Because of its high potency and selectivity, NAH-C4-GPKRIA was selected as our lead compound. According to the co-crystal structures of NTMT1 in complex with previous NTMT1 bisubstrate inhibitors,[24,25] we keep the tripeptide GPK intact in our design. The proposed **1**-**4** were synthesized in a convergent manner by reacting the primary amines (**7**–**8**) with α-bromo peptide on resin and followed by acid treatment as described before (Schemes 1).[23,25]

Inhibition Evaluation.

The inhibitory activities of compounds **1**-**4** against NTMT1 were evaluated in the SAH hydrolase (SAHH)-coupled fluorescence assay under the condition that both SAM and the peptide substrate GPKRIA were at their respective K_m values.[27] Previous studies demonstrated that NAH-C4-GPKRIA and NAH-C4-GPKR bisubstrate analogs containing a 4-C carbon link showed slightly higher potency than those with a 3-C atom linker.[25] However, the NAH-C3-GPKK bisubstrate analogue **1** with the 3-C atom linker ($K_{i,\ app}$ = 7 ± 1 nM) exhibited similar inhibition as its 4-C linker analogue **2** ($K_{i,\ app}$ = 5.0 ± 0.3 nM) (Table 1). Likewise, the NAH-C3-GPK bisubstrate analogue **3** with a 3-C carbon linker showed comparable inhibitory activity to compound **4** with a 4-C carbon linker, although the $K_{i,\ app}$ values of **3** and **4** were increased by 6–8 fold compared to **1** and **2** due to the shortened peptide moiety from a tetrapeptide to a tripeptide.

MALDI-MS Methylation Inhibition Assay.

For further validation, we evaluated the inhibitory effects of compound **1** on Nα-methylation progression with an orthogonal MALDI-MS methylation assay with 10 min preincubation (Figure 2A–B).[24,28] As NTMT1 can trimethylate the Nα-amine group of the substrate peptide GPKRIA in which the Nα-amine group is a primary amine, there would be mono-, di- and tri-methylation states for the methylated product in the methylation assay. The data was analyzed as described before.[28,29] Briefly, the relative fraction of each peptide was calculated from the areas of all of the relevant peaks for each component to provide the relative abundance. As the concentration of compound **1** increased, the trimethylated GPKRIA decreased along with the increased level of unmethylated GPKRIA (Figure 2B). For compound **1**, tri-methylation of GPKRIA was almost abolished at 200 nM (Figure 2B). Also, all the methylation products of GPKRIA were reduced to less than 10% at 100 nM of compound **1** (Figure 2A–B). Through calculating the relative reaction rate based on the relative abundance with three species methylated products, quantitative analysis of the data and fitting them with different compound concentrations yielded the $K_{i,\ app}$ of 15 ± 4 nM for **1** in the MS assay, which is comparable to the inhibitory activity in the fluorescence assay and further validated the potency of **1** for NTMT1.

Selectivity Assessment.

Next, we evaluated the selectivity of **1** for NTMT1 against a panel of several SAM-dependent methyltransferases, including two PKMTs (G9a and SETD7), and three PRMTs (PRMT1, PRMT3, and *Tb*PRMT7). We also include the SAHH, a coupling enzyme used in the fluorescence assay, which has a SAH binding site. Based on the results (Figure 2C), compound **1** retained the high selectivity to NTMT1, displaying more than 4,000-fold inhibition over other methyltransferases and SAHH.

Co-crystal Structure of Compound 1 (NAH-C3-GPKK) with NTMT1.

We obtained the X-ray crystal structure of the NTMT1-**1** complex (PDB ID: 6PVA) (Figure 3A), confirming its engagement with both cofactor and substrate binding sites of NTMT1. The structure of NTMT1-**1** overlaid well with the previously characterized co-crystal structure of bisubstrate inhibitor **NAH-C3-PPKRIA** (orange) with NTMT1 (PDB ID: 6DTN) (Figure 3B).[24] The NAH moiety of **1** exhibited almost the same binding mode to NTMT1 as the NAH portion of **NAH-C3-PPKRIA** (Figure 3B), which is nearly identical with SAH in the ternary complex of substrate peptide/SAH with NTMT1 (PDB ID: 5E1M).[8] Also, the peptide portion GPKK of **1** shows a similar binding mode compared with the PPKR peptide sequence in **NAH-C3-PPKRIA**. Specifically, the carbonyl oxygen of the first Gly forms a hydrogen bond with the side chain of Asn168 (Figure 3C). The second Pro residue inserts into the hydrophobic pocket formed by Leu31, Ile37, and Ile214, while the ε-amine group of the third Lys forms three hydrogen bonds with side chains of Asp177, Asp180, and Ser182.

Design of Affinity Probe 6.

As the last lysine is exposed to the solvent and its backbone forms interactions with NTMT1, we proposed that introduction of a clickable propargyl Gly (pG) to the C-terminus

of the peptide of **1**, as well as linking the biotin group with pG to obtain the biotinylated probe, would retain the interaction with NTMT1 and allow the derivatization to immobilize the probe on streptavidin beads. Biotin-streptavidin is a powerful non-covalent interaction with a high binding affinity (K_d = ~10^{-14} M).[30] The biotin-streptavidin system has been widely applied in many biological applications, including proteome profiling, bio-imaging, biotinylated antibodies, and protein purification.[30] Thus, probe **6** (NAH-C3-GPKK-biotin) was designed and synthesized for selectivity profiling (Scheme 2). To further confirm our design strategy, we also synthesized compound **5** (NAH-C3-GPKKpG) with a pG as the appendage (Scheme 2). Compound **5** demonstrated a comparable IC_{50} value (120 ± 20 nM) as compound **1** (150 ± 20 nM) in the SAHH-coupled fluorescence assay with a preincubation time of 10 minutes (Figure S1), supporting our design.

Chemical Proteomic Profiling with Immobilized Probe 6.

To investigate the optimal condition for the pull-down study, we first preincubated purified recombinant NTMT1 with immobilized probe **6** on streptavidin beads and eluted with a salt gradient in the elution buffer. NTMT1 was eluted off with the probe until the salt concentration reached 4 M NaCl, confirming strong interaction between **6** and NTMT1 (Figure S2A). To remove non-specific and weak binders, we chose the lysis buffer containing 700 mM NaCl to wash the immobilized beads after preincubation with HeLa cell lysates. In parallel, the streptavidin beads alone were used as a negative control to remove any nonspecific binders. NTMT1 was enriched by probe **6** but not in the bead alone (Figure 4A). Specific enrichment of NTMT1 was further confirmed by competition experiments using the free inhibitor **1** (Figure 4A, Probe 6+1), indicating that preincubation of the lysate with **1** blocked the interaction between probe **6** and NTMT1 and allowed for the identification of specific interacting partners for probe **6**. NTMT1 was not washed off by the buffer containing 700 mM NaCl (Figure 4A, 700 mM wash lanes in probe **6**), consistent with the tight interaction between NTMT1 and probe **6**.

Having confirmed the specific enrichment of NTMT1 by immobilized probe **6**, we performed an unbiased proteomic analysis of HeLa cell proteomics enriched by probe **6** through LC-MS/MS. We identified 23 proteins that were preferentially enriched by probe **6** with ≥6-fold change of ($\log_2$(probe **6**/probe **6** + **1**)) and ≥2 of confidence value (−$\log_{10}$(P-value)) for each identified protein (Figure 4B, Tables S1). Besides NTMT1, HemK methyltransferase family member 2 (HemK2, also known as KMT9[26,31] or N6AMT1[4,31]), and its binding partner Trm112, are the only identified methyltransferase subunits among the 23 identified proteins (Figure 4B–C), supporting the relatively high selectivity of the NTMT1 bisubstrate inhibitor. Interestingly, both NTMT1 and HemK2 were identified as differentially expressed genes potentially involved in glioma stem cell DNA hypermethylation (Figure 4D).[32] Other identified proteins included citron Rho-interacting kinase, small GTPases, RNA helicases, and ADP-ribosylation factors that have been involved in various pathways (Figure 4B–E). Notably, those identified proteins could either directly interact with the bait **6** or indirectly interact through NTMT1 or other possible targets. Validation of those interactions will be pursued through a pull-down study with purified NTMT1 or immunoprecipitation in the future. HemK2 and Trm112 forms a functional methyltransferase complex,[4,26,31] with HemK2 as the catalytic subunit and

Trm112 as an activator. The HemK2-Trm112 methyltransferase complex has a dual methyltransferase activity for either the protein lysine residue of histone H4 (named as KMT9) or glutamine residue of eRF1 (named as HemK2).[4,26] Although methyltransferase activity on a glutamine peptide (GGQSALR) is better than a lysine peptide (GKGGAKR), both sequences conform to a similar motif as G-Q/K-XXX-K/R.[4,26]

HemK2/KMT9 contains the SAM binding site and the substrate-binding site, while probe **6** consisted of a SAM analogue (NAH) and a peptide sequence GPKK containing two lysine residues. Thus, we hypothesized that the HemK2/KMT9 methyltransferase complex may bind with the NAH moiety or/and lysine-riched peptide sequence of the probe **6**. To validate this potential interaction, we performed a pull-down study of probe **6** with the HemK2-Trm112 complex in a similar manner as we did for NTMT1. HemK2 started to be eluted off from the probe when the salt concentration was at 500 mM to 1M NaCl (Figure S2B), demonstrating a direct interaction between probe **6** and HemK2. Then, we tested the inhibitory activity of the parent compound **1** for the HemK2/KMT9 complex with a preferred GGQ substrate peptide.[31] In Figure 5A–B, compound **1** exhibited a potent inhibition for HemK2/KMT9 with an IC_{50} value of 0.30 ± 0.03 μM at 0.6 μM of the complex, which is tenfold more potent than a general methyltransferase inhibitor sinefungin. When the concentration of the HemK2/KMT9 complex increased to 10 μM, compound **1** exhibited an IC_{50} value of 6.3 ± 0.8 μM, while a general methyltransferase inhibitor sinefungin only inhibited about 50% of activity at 100 μM (Figure 5C–D). As the IC_{50} value was approximately half of the enzyme concentration used in the assay in both cases and the inhibitor acted to titrate all of the enzyme molecules in the reaction, compound **1** served as a tight inhibitor for the HemK2/KMT9 complex.[33] To dissect if **1** targeted the active site of HemK2 or Trm112 or the interface between HemK2 and Trm112, we also assessed the inhibition for another methyltransferase complex mediated by Trm112, MettL5-Trm112.[34] Compound **1** exhibited no inhibition for MettL5-Trm112 complex at 1 μM (Figure 5E), suggesting that **1** directly targets HemK2.

To our knowledge, this is the first reported inhibitor for HemK2/KMT9 activity. Through monomethylation of histone H4 lysine 12 (H4K12), HemK2/KMT9 colocalized with H4K12me1 at gene promoters and regulated the gene transcription initiation.[26] Overexpression of HemK2/KMT9 was observed in prostate cancer cells, and knockdown of HemK2/KMT9 strongly reduced the proliferation of prostate cancer cell lines.[26] Besides, knockdown of HemK2/KMT9 severely inhibited the growth of prostate tumor xenografts.[26] Giving those emerging implications of HemK2/KMT9 in prostate cancers, compound **1** would provide a rational lead for the development of inhibitors targeting the HemK2/KMT9 methyltransferase complex to treat prostate cancers, as well as further improve the selectivity of NTMT1 inhibitors.

CONCLUSION

In summary, we have rationally developed an affinity probe **6** based on the parent compound **1** that is a highly potent and relatively selective bisubstrate inhibitor for NTMT1. Chemproteomic studies with probe **6** confirmed the high selectivity of the NTMT1 bisubstrate inhibitor since the HemK2/KMT9-Trm112 methyltransferase complex was the

only other methyltransferase that was enriched by probe **6**. Subsequent validation confirmed the parent inhibitor **1** was a tight inhibitor for the HemK2/KMT9 activity. As the first inhibitor for HemK2/KMT9, compound **1** would be a valuable probe and lead to developing potent inhibitors for HemK2/KMT9. Additionally, the future molecular mechanism investigation of **1** for HemK2/KMT9 would afford a solid basis to develop selective inhibitors for either methyltransferase.

METHODS

Chemistry General Procedures.

The reagents and solvents were purchased from commercial sources (Fisher) and used directly. Final compounds were purified on preparative high-pressure liquid chromatography (RP-HPLC) was performed on Agilent 1260 Series system. Systems were run with 0–20% methanol/water gradient with 0.1% TFA. Matrix-assisted laser desorption ionization mass spectra (MALDI-MS) data were acquired in positive-ion mode using a Sciex 4800 MALDI TOF/TOF MS. The peptides were synthesized using a CEM Liberty Blue Automated Microwave Peptide Synthesizer with the manufacturer's standard coupling cycles at 0.1 mmol scales. The purity of the final compounds was confirmed by Agilent 1260 Series HPLC system. Systems were run with a 0–40% methanol/water gradient with 0.1% TFA. All the purity of target compounds showed >95%.

α-bromo peptides (G*PK, G*PKK, G*PKKpG).—To the solution of bromo acetic acid (139 mg, 1 mmol) in DMF(3 mL), DIC (155 μL, 1 mmol) was added and the solution was stirred for 20min at r.t. Then added the solution into the peptides on the resin (0.1 mmol). The mixture was shaken overnight at r.t. The suspension was filtered, and the resin was washed with DMF (3 ml × 3). Test cleavage (TFA: TIPS: H_2O = 95:2.5:2.5) was performed to monitor the progress of the reaction.

NAH-C3-GPKK (**1**). To a suspension of G*PKK on the resin (0.1 mmol) in DMF (3 mL) was added compound **7** (91 mg, 0.15 mmol) and DIPEA (26 μL, 0.15 mmol). The mixture was shaken at room temperature overnight. The suspension was filtered, and the resin was subsequently washed with DMF (3 mL × 3), MeOH (3 mL × 3), and CH_2Cl_2 (3 mL × 3). The peptide conjugates were cleaved from the resin in the presence of a cleavage cocktail (10 mL) containing trifluoroacetic acid (TFA)/2,2'-(Ethylenedioxy)-diethanethiol (DODT) / triisopropylsilane (TIPS) /water (94:2.5:1:2.5 v/v) at room temperature for 4–5 h and resin was rinsed with a small amount of TFA. Volatiles were removed under N_2 and the residue was precipitated with 10 vol. cold anhydrous ether, and collected by centrifugation. The supernatant was discarded and the pellet was washed with chilled ether and air-dried. The white precipitate was dissolved in ddH_2O and purified by reverse phase HPLC using a waters system with an XBridge (BEH C18, 5 μm, 10 × 250 mm) column with 0.1% TFA in water (A) and MeOH (B) as the mobile phase with monitoring at 214 nm and 254 nm. MALDI-MS (positive) m/z: calcd for $C_{36}H_{63}+N_{14}O_9$ $[M + H]^+$ m/z 835.4902, found m/z 835.5424.

NAH-C4-GPKK (**2**). The compound was prepared according to the procedure for NAH-C3-GPKK (**1**) and purified by reverse-phase HPLC. MALDI-MS (positive) m/z: calcd for $C_{37}H_{65}N_{14}O_9$ $[M + H]^+$ m/z 849.5059, found m/z 849.7359.

NAH-C3-GPK (**3**). The compound was prepared according to the procedure for NAH-C3-GPKK (**1**) and purified by reverse-phase HPLC. MALDI-MS (positive) m/z: calcd for $C_{30}H_{51}N_{12}O_8$ $[M + H]^+$ m/z 707.3953, found m/z 707.5096.

NAH-C4-GPK (**4**). The compound was prepared according to the procedure for NAH-C3-GPKK (**1**) and purified by reverse-phase HPLC. MALDI-MS (positive) m/z: calcd for $C_{31}H_{53}N_{12}O_8$ $[M + H]^+$ m/z 721.4109, found m/z 721.5273.

NAH-C3-GPKKpG (**5**). The compound was prepared according to the procedure for NAH-C3-GPKK (**1**) and purified by reverse-phase HPLC. MALDI-MS (positive) m/z: calcd for $C_{41}H_{68}N_{15}O_{10}$ $[M + H]^+$ m/z 930.5274, found m/z 930.6367.

NAH-C3-GPKK-Biotin (**6**). To a suspension of G*PKK-pG on the resin (0.05 mmol) in DMF (2 mL) was added compound **7** (45 mg, 0.075 mmol) and DIPEA (13 μL, 0.075 mmol). The mixture was shaken at room temperature overnight. The suspension was filtered, and the resin was subsequently washed with DMF (3 mL × 3), MeOH (3 mL × 3), and CH_2Cl_2 (3 mL × 3). Then $CuSO_4 \cdot 5H_2O$ (25 mg, 0.1 mmol), sodium ascorbate (20 mg, 0.1mmol), and DMF (2 mL) were mixed with the resin. The mixture was shaken overnight at room temperature. The cleavage and purification of the conjugate were conducted according to the procedure for NAH-C3-GPKK (**1**). MALDI-MS (positive) m/z: calcd for $C_{59}H_{100}N_{21}O_{15}S$ $[M + H]^+$ m/z 1374.7428, found m/z 1375.1959.

Protein Expression and Purification.

Expression and purification of NTMT1, G9a, SETD7, PRMT1, PRMT3, *Tb*PRMT7, HemK2-Trm112, and MettL5-Trm112 were performed as previously described.[8,25,31,34–37]

NTMT1 Biochemical Assays.

A fluorescence-based SAHH-coupled assay was applied to study the IC_{50} and $K_{i,app}$ values of compounds with both SAM and the peptide substrate at their K_m values. For 10min pre-incubation, the methylation assay was performed under the following conditions in a final well volume of 40 μL: 25 mM Tris (pH = 7.5), 50 mM KCl, 0.01% Triton X-100, 5 μM SAHH, 0.1 μM NTMT1, 3 μM SAM, and 10 μM ThioGlo4. The inhibitors were added at concentrations ranging from 0.15 nM to 10 μM. After 10 min incubation, reactions were initiated by the addition of 0.5 μM GPKRIA peptide. For 120min pre-incubation, NTMT1 and compounds were pre-incubated for 120min. Then the pre-incubation mixture was added into reaction mixture: 25 mM Tris (pH = 7.5), 50 mM KCl, 0.01% Triton X-100, 5 μM SAHH, 3 μM SAM, and 10 μM ThioGlo4. The reactions were initiated by the addition of 0.5 μM GPKRIA peptide. Fluorescence was monitored on a BMG CLARIOstar microplate reader with excitation of 400 nm and emission of 465 nm. Data were processed by using GraphPad Prism software 7.0.

Selectivity Assays.

The selectivity studies of G9a, SETD7, PRMT1, PRMT3, *Tb*PRMT7, and SAHH were performed as previously described.[24,25,38]

MALDI-MS Methylation Inhibition Assay.

The methylation inhibition study of compound **1** with NTMT1 was performed as previously described.[25]

HemK2-Trm112 Methylation Inhibition Assay.

The methylation inhibition assays of HemK2-Trm112 was performed in a 20 μL reaction mixture containing 20 mM Tris-HCl (pH 8.0), 50 mM NaCl, 1 mM DTT and 20 μM SAM at 37°C, using high or low enzyme concentrations (10 μM or 0.6 μM), varied concentrations of eRF1 peptide (residues 179–183: KHGRGGQSALRFARL) (10 μM or 400 μM) and of compound 1 (NAH-C3-GPKK) or Sinefungin. The SAM-dependent methylation activity was measured by the Promega bioluminescence assay.[31]

MettL5-Trm112 Methylation Inhibition Assay.

The methylation inhibition assays of MettL5-Trm112 was carried out at room temperature (~22°C) for 20 min in a 20 μL reaction mixture containing 20 mM Tris-HCl (pH 8.0), 1 mM DTT, 20 μM SAM, 0.2 μM purified MettL5-Trm112 complex, 10 μM RNA (5'-UCGUA**A**CAAGGUUU-3').[34] Various concentrations (0–1 μM) of compound **1** (NAH-C3-GPKK) were added. The by-product SAH of methylation reaction was measured by the Promega bioluminescence assay.[31]

Pull-down Assay.

Probe **6** (100 μL, 100 μM) was incubated with 50 μL streptavidin resin overnight in 20mM Tris, 50 mM KCl, pH=7.5. After removing any unbounded probe, purified NTMT1 was incubated with the probe-bound resin in 20 mM Tris, 50 mM KCl, 1 mM DTT, pH=7.5 for 4 h. Likewise, purified HemK2-Trm112 protein complex was incubated with the probe-bound resin in 20 mM HEPES, 300 mM NaCl, 0.5 mM TCEP, 5% Glycerol, pH 8.0 for 4 h. Then the resin was washed with 1 mL (20x resin volume) of respective incubation buffer multiple times until no protein was detected via Nanodrop (Thermo Scientific™). Different concentrations of the salt solution (500 mM, 1 M, 2 M, 4 M NaCl) were used to elute NTMT1 or HemK2-Trm112 protein complex. The salt concentration was changed until protein concentration of precedent elution was close to 0 mg/mL according to Nanodrop (Thermo Scientific™).

HeLa cells (~ 6×10^8 cells/mL) were lysed with fresh IP buffer containing 25 mM Tris, 150 mM NaCl, 1% NP-40, 1 mM EDTA, 5% glycerol, protease inhibitor (Halt ™ protease inhibitor cocktail) pH 7.4. The cell suspension was incubated in rotation for 1 h at 4 °C and centrifuged at 15,000 g for 25 min at 4 °C to obtain the supernatant. The concentration of protein was determined with a BCA protein assay. The HeLa cell lysate was incubated with probe-covered resin (50 μL) overnight. For the competitor pulldown assay, competitor compound **1** (10 mM, 5 μL) was treated to the cell lysate first and incubate with compound-

covered resin overnight. Resin alone was used as a negative control. Washed the resin five times with 1 mL (20x resin volume) IP buffer five times to remove the nonbounded proteins. The resin was then washed with 1 mL 700 mM NaCl more than five times to remove the weak binding proteins until protein concentration of washing elution was close to 0 mg/mL via Nanodrop (Thermo Scientific™). 1X SDS loading buffer was added and the resin was boiled for 5 min at 95 °C to elute proteins on it. Protein samples (10 μL) were loaded on 12.5 % SDS-PAGE gels and run at 120 V until the proteins come to the edge of the gel. Coomassie blue was used to stain the gels. Proteins on the gel were transferred to the PVDF membrane. After 5% milk blocking, the membrane was incubated with anti-NTMT1 (1:1000 dilution in 5% BSA in TBST buffer, Cell signaling #13432) at 4 °C overnight. Anti-rabbit IgG, HRP-linked antibody (1:1000 dilution in 5% BSA in TBST buffer, Cell signaling #7074) was incubated at 4 °C for 1 h. The membrane was developed with ECL substrate (BIO-RAD #1705061) and imaged with a Proteinsimple FluorChem R.

Protein samples (10 μL) were loaded on 12.5 % SDS-PAGE gels and run at 120 V for 10 min. Protein bands were cut and submitted to the Laboratory for Biological Mass Spectrometry at Indiana University for LC-MS/MS.

Co-crystallization and Structure Determination.

The co-crystallization and structure determination of compound **1** with NTMT1 were performed as previously described.[24,25] Purified NTMT1 (30 mg/mL) was mixed with **1** at a 1:2 molar ratio, and the mixture was incubated overnight at 4°C. Using the hanging-drop vapor diffusion method and incubation at 20°C, the crystals of **1** were grown in 1.5 M lithium sulfate, 0.1 M sodium HEPES (pH = 7.5). The crystals were then harvested and flash frozen in liquid nitrogen. Data were collected on a single crystal at 12.0 keV at the GM/CA-CAT ID-D beamline at the Advanced Photon Source, Argonne National Laboratory. The data were processed (Table S2) and the structure was solved as previously described.[24,25]

Supplementary Material

Refer to Web version on PubMed Central for supplementary material.

ACKNOWLEDGMENT

This research used resources of the Advanced Photon Source, a U.S. Department of Energy (DOE) Office of Science User Facility operated for the DOE Office of Science by Argonne National Laboratory under Contract No. DE-AC02-06CH11357. We also thank supports from the Department of Medicinal Chemistry and Molecular Pharmacology (RH) and the Department of Biological Sciences (NN) at Purdue University. We thank C. Woodcock for previous invovlment in purification of human HemK2-Trm112 complex. We thank the Laboratory for Biological Mass Spectrometry at Indiana University for LC-MS/MS analysis and raw data process.

Funding

The authors acknowledge the support from NIH grants R01GM117275 (RH), 1R01GM127896 (NN), 1R01AI127793 (NN), R35GM134744 (XC), and P30 CA023168 (Purdue University Center for Cancer Research). XC, a CPRIT Scholar in Cancer Research, thanks the support of Cancer Prevention and Research Institute of Texas (RR160029). GM/CA@APS beamline has been funded in whole or in part with Federal funds from the National Cancer Institute (ACB-12002) and the National Institute of General Medical Sciences (AGM-12006).

ABBREVIATIONS

NTMT	protein N-terminal methyltransferase
SAM	*S*-adenosyl-L-methionine
SAH	S-adenosyl-L-homocysteines
SAHH	SAH hydrolase
MT	methyltransferase
PKMT	protein lysine methyltransferase
PRMT	protein arginine methyltransferase
G9a	euchromatic histone-lysine N-methyltransferase 2
SETD7	SET domain-containing protein 7
***Tb*PRMT7**	*Trypanosoma brucei* protein arginine methyltransferase 7
HemK2	HemK methyltransferase family member 2
MettL5	methyltransferase-like protein 5
rt	room temperature
TFA	trifluoroacetic acid

REFERENCES

(1). Luo M (2018) Chemical and Biochemical Perspectives of Protein Lysine Methylation. Chem. Rev 118, 6656–6705. [PubMed: 29927582]

(2). Kaniskan HU, Martini ML, Jin J (2018) Inhibitors of Protein Methyltransferases and Demethylases. Chem. Rev 118, 989–1068. [PubMed: 28338320]

(3). Jarrold J, Davies CC (2019) PRMTs and Arginine Methylation : Cancer ‘s Best-Kept Secret? Trends Mol. Med 25, 993–1009. [PubMed: 31230909]

(4). Gao J, Wang B, Yu H, Wu G, Wan C, Liu W (2020) Structural Insight into HEMK2-TRMT112 Mediated Glutamine Methylation. Biochem. J 477, 3833–3838. [PubMed: 32969463]

(5). Tooley CES, Petkowski JJ, Muratore-Schroeder TL, Balsbaugh JL, Shabanowitz J, Sabat M, Minor W, Hunt DF, Macara IG (2010) NRMT Is an Alpha-N-Methyltransferase That Methylates RCC1 and Retinoblastoma Protein. Nature 466, 1125–1128. [PubMed: 20668449]

(6). Feng Y, Hadjikyriacou A, Clarke SG (2014) Substrate Specificity of Human Protein Arginine Methyltransferase 7 (PRMT7): The Importance of Acidic Residues in the Double e Loop. J. Biol. Chem 289, 32604–32616. [PubMed: 25294873]

(7). Del Rizzo PA, Trievel RC (2014) Molecular Basis for Substrate Recognition by Lysine Methyltransferases and Demethylases. Biochim. Biophys. Acta - Gene Regul. Mech 1839, 1404–1415.

(8). Dong C, Mao Y, Tempel W, Qin S, Li L, Loppnau P, Huang R, Min J (2015) Structural Basis for Substrate Recognition by the Human N-Terminal Methyltransferase 1. Genes Dev. 29, 2343–2348. [PubMed: 26543161]

(9). Jakobsson ME, Małecki JM, Halabelian L, Nilges BS, Pinto R, Kudithipudi S, Munk S, Davydova E, Zuhairi FR, Arrowsmith CH, Jeltsch A, Leidel SA, Olsen JV, Falnes P (2018) The Dual

Methyltransferase METTL13 Targets N Terminus and Lys55 of EEF1A and Modulates Codon-Specific Translation Rates. Nat. Commun 9, 3411. [PubMed: 30143613]

(10). Frankel A, Yadav N, Lee J, Branscombe TL, Clarke S, Bedford MT (2002) The Novel Human Protein Arginine N-Methyltransferase PRMT6 Is a Nuclear Enzyme Displaying Unique Substrate Specificity. J. Biol. Chem 277, 3537–3543. [PubMed: 11724789]

(11). Liu X, Wang L, Li H, Lu X, Hu Y, Yang X, Huang C, Gu D (2014) Coactivator-Associated Arginine Methyltransferase 1 Targeted by MiR-15a Regulates inflammation in Acute Coronary Syndrome. Atherosclerosis 233, 349–356. [PubMed: 24530761]

(12). Wang SM, Dowhan DH, Muscat GEO (2019) Epigenetic Arginine Methylation in Breast Cancer : Emerging Therapeutic Strategies. J. Mol. Endocrinol 62, R223–R227. [PubMed: 30620710]

(13). Tsai W, Niessen S, Goebel N, Yates JR, Guccione E, Montminy M (2013) PRMT5 Modulates the Metabolic Response to Fasting Signals. Proc. Natl. Acad. Sci. U.S.A 110, 8870–8875. [PubMed: 23671120]

(14). Wu R, Yue Y, Zheng X, Li H (2015) Molecular Basis for Histone N-Terminal Methylation by NRMT1. Genes Dev. 29, 2337–2342. [PubMed: 26543159]

(15). Dai X, Rulten SL, You C, Caldecott KW, Wang Y (2015) Identification and Functional Characterizations of N-Terminal α- N -Methylation and Phosphorylation of Serine 461 in Human Poly(ADP-Ribose) Polymerase 3. J. Proteome Res 14, 2575–2582. [PubMed: 25886813]

(16). Sathyan KM, Fachinetti D, Foltz DR (2017) α-Amino Trimethylation of CENP-A by NRMT Is Required for Full Recruitment of the Centromere. Nat. Commun 8, 1–15. [PubMed: 28232747]

(17). Dai X, Otake K, You C, Cai Q, Wang Z, Masumoto H, Wang Y (2013) Identification of Novel α-N-Methylation of CENP-B That Regulates Its Binding to the Centromeric DNA. J. Proteome Res 12, 4167–4175. [PubMed: 23978223]

(18). Cai Q, Fu L, Wang Z, Gan N, Dai X, Wang Y (2014) α-N-Methylation of Damaged DNA-Binding Protein 2 (DDB2) and Its Function in Nucleotide Excision Repair. J. Biol. Chem 289, 16046–16056. [PubMed: 24753253]

(19). Bailey AO, Panchenko T, Sathyan KM, Petkowski JJ, Pai P-J, Bai DL, Russell DH, Macara IG, Shabanowitz J, Hunt DF, Black BE, Foltz DR (2013) Posttranslational Modification of CENP-A Influences the Conformation of Centromeric Chromatin. Proc. Natl. Acad. Sci 110, 11827–11832. [PubMed: 23818633]

(20). Bonsignore LA, Tooley JG, Van Hoose PM, Wang E, Cheng A, Cole MP, Schaner Tooley CE (2015) NRMT1 Knockout Mice Exhibit Phenotypes Associated with Impaired DNA Repair and Premature Aging. Mech. Ageing Dev 146–148, 42–52.

(21). Bonsignore LA, Butler JS, Klinge CM, Tooley CES, Schaner Tooley CE (2015) Loss of the N-Terminal Methyltransferase NRMT1 Increases Sensitivity to DNA Damage and Promotes Mammary Oncogenesis. Oncotarget 6, 12248–12263. [PubMed: 25909287]

(22). Zhang G, Richardson SL, Mao Y, Huang R (2015) Design, Synthesis, and Kinetic Analysis of Potent Protein N-Terminal Methyltransferase 1 Inhibitors. Org. Biomol. Chem 13, 4149–4154. [PubMed: 25712161]

(23). Zhang G, Huang R (2016) Facile Synthesis of SAM-Peptide Conjugates through Alkyl Linkers Targeting Protein N-Terminal Methyltransferase 1. RSC Adv. 6, 6768–6771. [PubMed: 27588169]

(24). Chen D, Dong G, Noinaj N, Huang R (2019) Discovery of Bisubstrate Inhibitors for Protein N-Terminal Methyltransferase 1. J. Med. Chem 62, 3773–3779. [PubMed: 30883119]

(25). Chen D, Dong C, Dong G, Srinivasan K, Min J, Noinaj N, Huang R (2020) Probing the Plasticity in the Active Site of Protein N-Terminal Methyltransferase 1 Using Bisubstrate Analogues. J. Med. Chem 63, 8419–8431. [PubMed: 32605369]

(26). Metzger E, Wang S, Urban S, Willmann D, Schmidt A, Offermann A, Allen A, Sum M, Obier N, Cottard F, Ulferts S, Preca BT, Hermann B, Maurer J, Greschik H, Hornung V, Einsle O, Perner S, Imhof A, Jung M, Schüle R (2019) KMT9 Monomethylates Histone H4 Lysine 12 and Controls Proliferation of Prostate Cancer Cells. Nat. Struct. Mol. Biol 26, 361–371. [PubMed: 31061526]

(27). Allali-hassani A, Wasney GA, Siarheyeva A, Hajian T, Vedadi M, Cheryl H (2012) Fluorescence-Based Methods for Screening Writers and Readers of Histone Methyl Marks. J. Biomol. Screening 17, 71–84.

(28). Richardson SL, Mao Y, Zhang G, Hanjra P, Peterson DL, Huang R (2015) Kinetic Mechanism of Protein N-Terminal Methyltransferase 1. J. Biol. Chem 290, 11601–11610. [PubMed: 25771539]

(29). Richardson SL, Hanjra P, Zhang G, Mackie BD, Peterson DL, Huang R (2015) A Direct, Ratiometric, and Quantitative MALDI-MS Assay for Protein Methyltransferases and Acetyltransferases. Anal. Biochem 478, 59–64. [PubMed: 25778392]

(30). Dundas CM, Demonte D, Park S (2013) Streptavidin-Biotin Technology: Improvements and Innovations in Chemical and Biological Applications. Appl. Microbiol. Biotechnol 97, 9343–9353. [PubMed: 24057405]

(31). Woodcock CB, Yu D, Zhang X, Cheng X (2019) Human HemK2/KMT9/N6AMT1 Is an Active Protein Methyltransferase, but Does Not Act on DNA in Vitro, in the Presence of Trm112. Cell Discov. 5, 4–6. [PubMed: 30652025]

(32). Baysan M, Woolard K, Bozdag S, Riddick G, Kotliarova S, Cam MC, Belova GI, Ahn S, Zhang W, Song H, Walling J, Stevenson H, Meltzer P, Fine HA (2014) Micro-Environment Causes Reversible Changes in DNA Methylation and mRNA Expression Profiles in Patient-Derived Glioma Stem Cells. PLoS One 9, e94045. [PubMed: 24728236]

(33). Morrison JF (1982) The Slow-Binding and Slow, Tight-Binding Inhibition of Enzyme-Catalysed Reactions. Trends Biochem. Sci 7, 102–105.

(34). Yu D, Kaur G, Blumenthal RM, Zhang X, Cheng X (2021) Enzymatic Characterization of Three Human RNA Adenosine Methyltransferases Reveals Diverse Substrate Affinities and Reaction Optima. J. Biol. Chem 296, 100270. [PubMed: 33428944]

(35). Wu H, Min J, Lunin VV, Antoshenko T, Dombrovski L, Zeng H, Allali-Hassani A, Campagna-Slater V, Vedadi M, Arrowsmith CH, Plotnikov AN, Schapira M (2010) Structural Biology of Human H3K9 Methyltransferases. PLoS One 5, e8570. [PubMed: 20084102]

(36). Del Rizzo PA, Dirk LMA, Strunk BS, Roiko MS, Brunzelle JS, Houtz RL, Trievel RC (2010) SET7 / 9 Catalytic Mutants Reveal the Role of Active Site Water Molecules in Lysine Multiple Methylation. J. Biol. Chem 285, 31849–31858. [PubMed: 20675860]

(37). Debler EW, Jain K, Warmack RA, Feng Y, Clarke SG, Blobel G (2016) A Glutamate / Aspartate Switch Controls Product Specificity in a Protein Arginine Methyltransferase. Proc. Natl. Acad. Sci. U.S.A 113, 1–6.

(38). Chen D, Li L, Diaz K, Iyamu ID, Yadav R, Noinaj N, Huang R (2019) Novel Propargyl-Linked Bisubstrate Analogues as Tight-Binding Inhibitors for Nicotinamide N-Methyltransferase. J. Med. Chem 62, 10783–10797. [PubMed: 31724854]

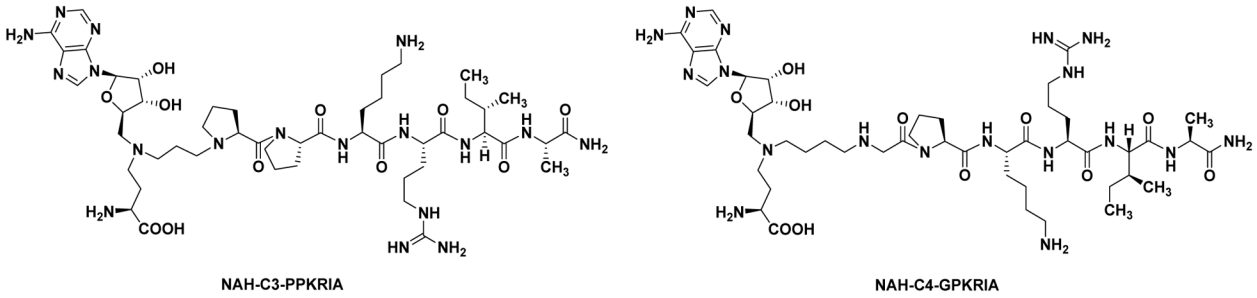

Figure 1.
Chemical structures of NTMT1 bisubstrate inhibitors.

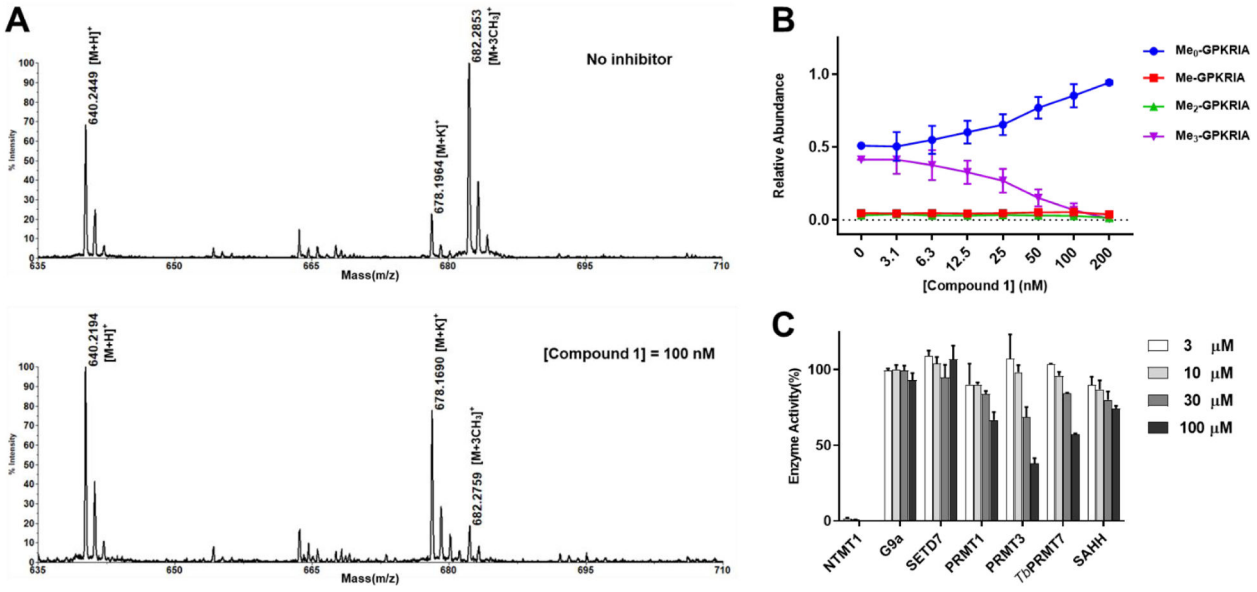

Figure 2.

Methylation inhibition and selectivity study for **1**. (A) Representative MS results of MALDI-MS methylation inhibition assay for **1**. $[GPKRIA+H]^+$ = 640, $[GPKRIA+K]^+$ = 678, $[GPKRIA+3CH_3]^+$ = 682; (B) Quantification of methylation progression of GPKRIA by NTMT1 in presence of various concentrations of **1** at 20 min (n=2). (C) Selectivity of **1** against several methyltransferases and SAH hydrolase (n=2).

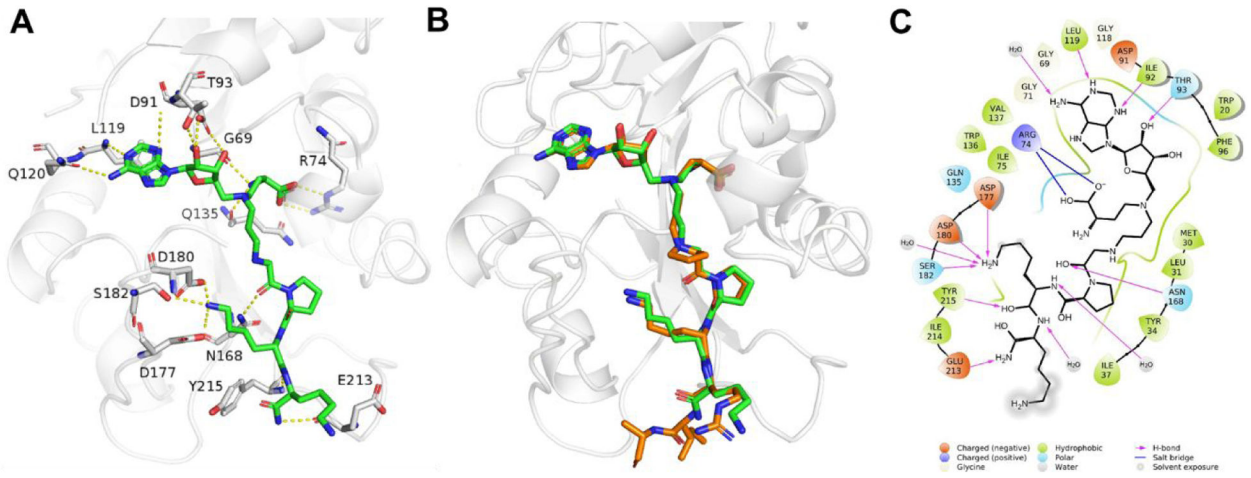

Figure 3.

X-ray co-crystal structure of NTMT1- **1** (PDB ID: 6PVA). (A) Zoomed view of interactions of **1** (green) complex with NTMT1(gray). H-bond interactions are shown in yellow dotted lines; (B) Structural alignment of NTMT1(gray)-**1** (green) complex with NTMT1-**NAH-C3-PPKRIA** (orange) binary complex (PDB ID: 6DTN); (C) 2D interaction diagram (Schrödinger Maestro) of **1** with NTMT1.

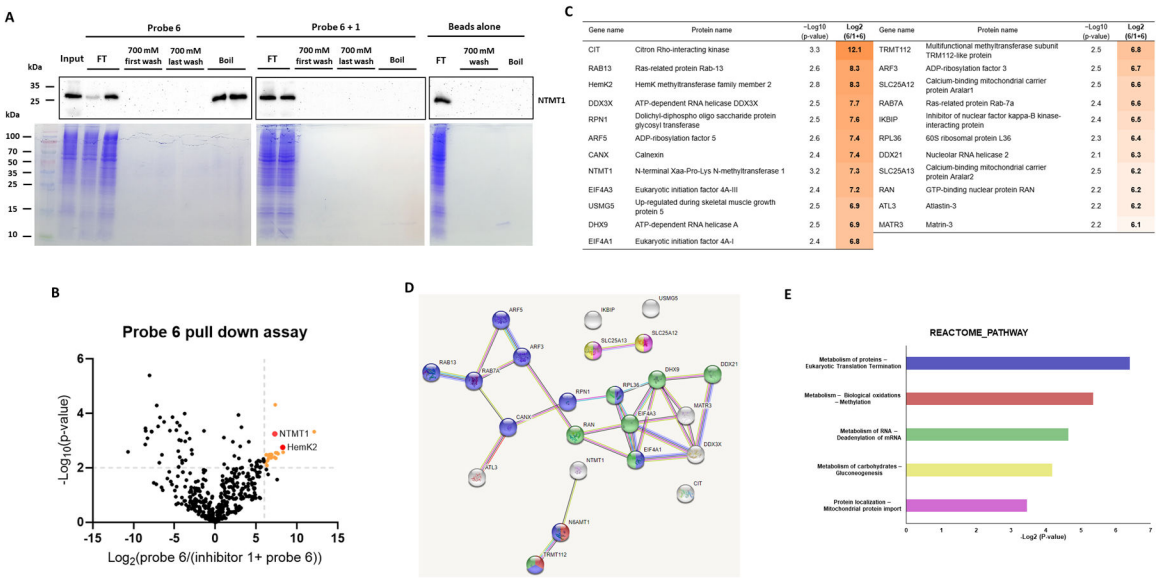

Gene name	Protein name	−Log10 (p-value)	Log2 (6/1+6)
CIT	Citron Rho-interacting kinase	3.3	12.1
RAB13	Ras-related protein Rab-13	2.6	8.3
HemK2	HemK methyltransferase family member 2	2.8	8.3
DDX3X	ATP-dependent RNA helicase DDX3X	2.5	7.7
RPN1	Dolichyl-diphospho oligo saccharide protein glycosyl transferase	2.5	7.6
ARF5	ADP-ribosylation factor 5	2.6	7.4
CANX	Calnexin	2.4	7.4
NTMT1	N-terminal Xaa-Pro-Lys N-methyltransferase 1	3.2	7.3
EIF4A3	Eukaryotic initiation factor 4A-III	2.4	7.2
USMG5	Up-regulated during skeletal muscle growth protein 5	2.5	6.9
DHX9	ATP-dependent RNA helicase A	2.5	6.9
EIF4A1	Eukaryotic initiation factor 4A-I	2.4	6.8
TRMT112	Multifunctional methyltransferase subunit TRM112-like protein	2.5	6.8
ARF3	ADP-ribosylation factor 3	2.5	6.7
SLC25A12	Calcium-binding mitochondrial carrier protein Aralar1	2.5	6.6
RAB7A	Ras-related protein Rab-7a	2.4	6.6
IKBIP	Inhibitor of nuclear factor kappa-B kinase-interacting protein	2.4	6.5
RPL36	60S ribosomal protein L36	2.3	6.4
DDX21	Nucleolar RNA helicase 2	2.1	6.3
SLC25A13	Calcium-binding mitochondrial carrier protein Aralar2	2.5	6.2
RAN	GTP-binding nuclear protein RAN	2.2	6.2
ATL3	Atlastin-3	2.2	6.2
MATR3	Matrin-3	2.2	6.1

Figure 4.

Competitive chemical proteomic profiling with immobilized probe **6**. (A) Probe **6** enriches NTMT1 from HeLa cell lysates. Western blot analysis of NTMT1 in HeLa cells lysates with the presence or absence of NTMT1 inhibitor **1** which were incubated with immobilized probe **6**. The NTMT1 immunoblots of the flow-through (FT), 700 mM NaCl wash, and boiled beads with anti-NTMT1 antibody (Cell signaling #13432) were shown. (B) The volcano plot of $-\text{Log}_{10}$(p-value) vs Log_2(probe/competition) for proteins identified via LC-MS/MS using probe **6** and inhibitor **1**. Statistically significant interactors for probe **6** were defined as protein hits with fold change = Log_2(Intensity (probe **6**)/Intensity (inhibitor **1** + probe **6**)) ≥ 6 and a confidence value = $-\log_{10}$(P-value) ≥ 2. Positions of NTMT1 and HemK2 are indicated in the plot by red circles. (C) The list of proteins that show statistically significant enrichment with probe **6** from HeLa cells. The third column shows confidence values ($-\log_{10}$(P-value)), and the fourth column shows enrichment scores. (D) STRING network of significant interactors for probe **6**. The STRING database was used to generate a network with these interactors. Each circle (node) represents a protein. Each line between the nodes represents a detected connection between two proteins in the STRING database. (E) Reactome pathway analysis of significant interactors for probe **6**. The interactors involved pathways were analyzed by STRING and DAVID databases. Proteins involve in each pathway were showed in the same color (Figure 4D) as the pathway bar. Proteins showed in white were not involved in any pathway from these two databases.

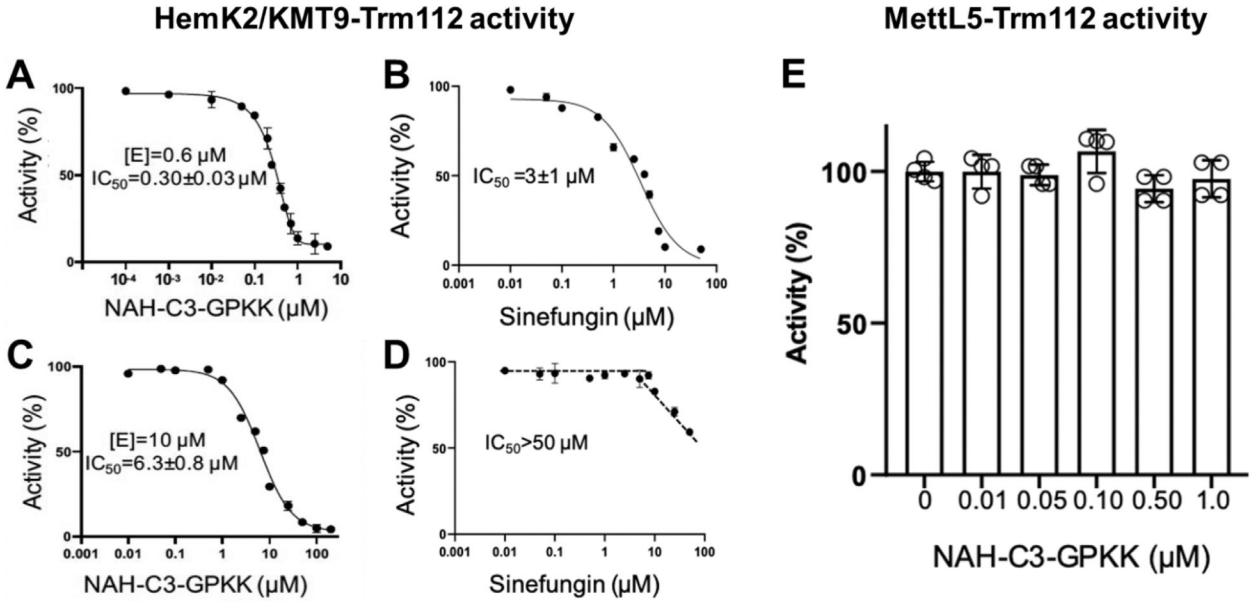

Figure 5.

(A) and (B) IC_{50} curves of compound **1** (NAH-C3-GPKK) and sinefungin for HemK2/KMT9-Trm112 activity on a GGQ peptide (n=3). The concentration of the HemK2/KMT9-Trm112 complex was 0.6 μM; (C) and (D) IC_{50} curves of compound **1** (NAH-C3-GPKK) and sinefungin for HemK2/KMT9-Trm112 activity on a GGQ peptide (n=3). The concentration of the complex was 10 μM; (E) compound **1** (NAH-C3-GPKK) for MettL5-Trm112 activity (n=3). The concentration of the complex was 0.2 μM.

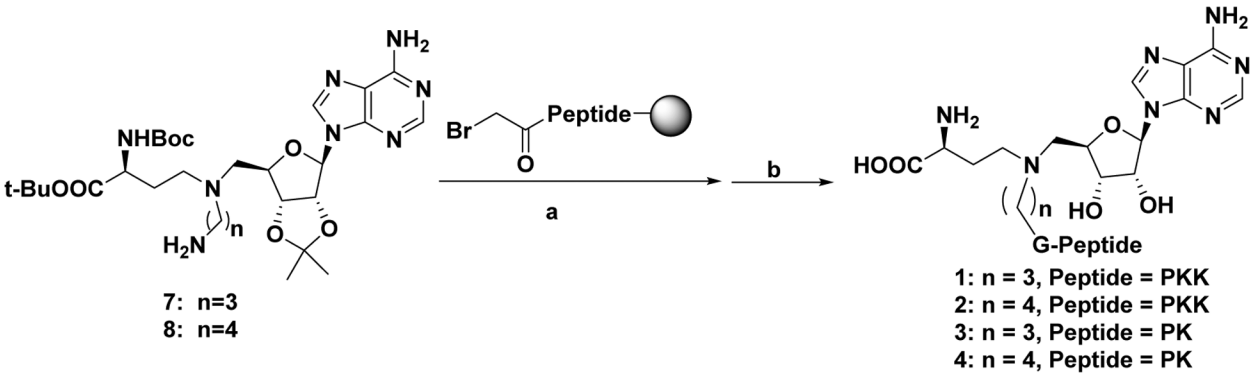

Scheme 1. Synthetic route for compounds 1–4.[a]

[a]Reagents and conditions: (a) α-bromo peptides on resin, DIPEA, DMF, r.t.; (b) TFA: DODT: H_2O: TIPS = 94: 2.5: 2.5: 1.

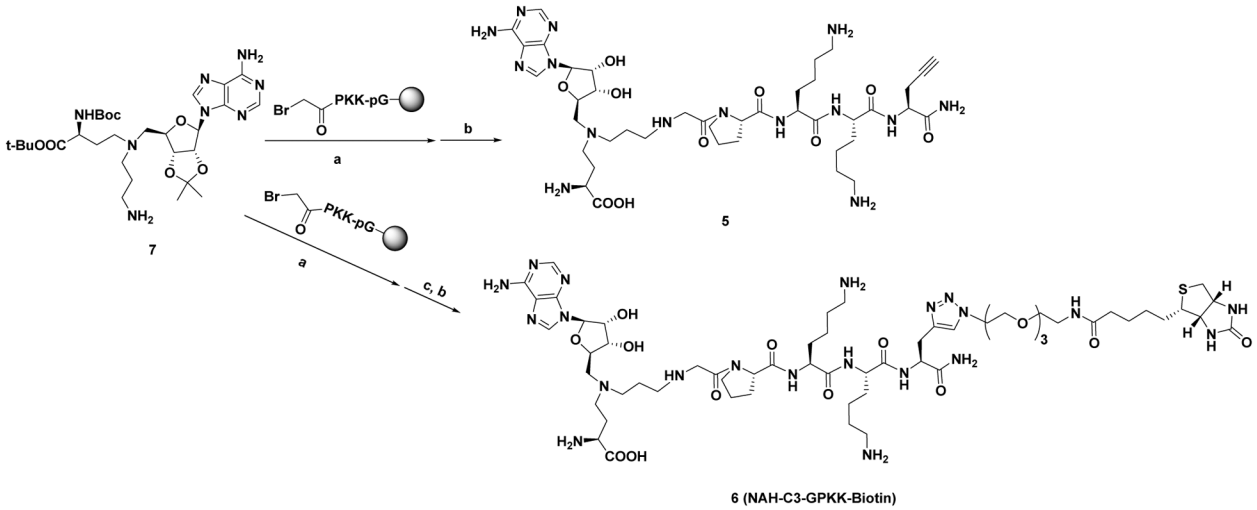

Scheme 2. Synthetic route for compounds 5 and 6.[a]

[a]Reagents and conditions: (a) DIPEA, DMF, r.t.; (b) TFA: DODT: H_2O: TIPS = 94: 2.5: 2.5: 1; (c) Biotin TEG-azide, $CuSO_4$, sodium ascorbate, DMF, r.t.

Table 1.

NTMT1 inhibition evaluation of bisubstrate analogues

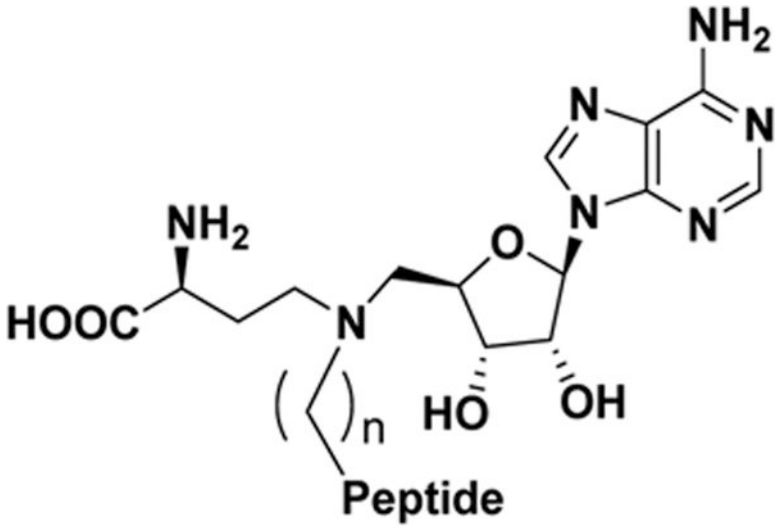

Compound ID	Peptide	n	$K_{i,\ app}$ (nM)
1 (NAH-C3-GPKK)	GPKK	3	7 ± 1
2 (NAH-C4-GPKK)	GPKK	4	5.0 ± 0.3
3 (NAH-C3-GPK)	GPK	3	41 ± 4
4 (NAH-C4-GPK)	GPK	4	44 ± 3